

Anisotropic roughness scattering at a heterostructure interface

Y. Tokura, T. Saku, S. Tarucha, and Y. Horikoshi

NTT Basic Research Laboratories, Musashino-shi, Tokyo 180, Japan

(Received 6 July 1992; revised manuscript received 30 September 1992)

Anisotropic Hall mobilities of a two-dimensional electron gas are observed in modulation-doped $\text{Al}_x\text{Ga}_{1-x}\text{As}/\text{GaAs}$ heterostructures grown by molecular-beam epitaxy on a (001) GaAs substrate. The mobility in the $[\bar{1}10]$ direction is larger than that in the $[110]$ direction. An anisotropic interface roughness is proposed to account for the observed anisotropic Hall mobilities. The dependences of the anisotropic mobilities on the electron concentration are explained well by the theoretical calculation, which assumes the existence of interface islands longer in the $[\bar{1}10]$ direction than in the $[110]$ direction. This assumption is consistent with previous reports on *in situ* measurement of growing surfaces by scanning tunneling microscope and electron diffraction.

The dominant electron-scattering process in modulation-doped structures at low temperatures is thought to be ionized-impurity scattering.¹ When the ionized impurities are far from the conducting channel, there appears a new regime of scattering, where interface-roughness scattering competes with ionized-impurity scattering. Although the situation is quite similar to a silicon metal-oxide-semiconductor structure (Refs. 2–5), the properties of the “roughness” are quite different. In the heterostructure, the height of the roughness is the order of monolayers and the spatial distribution of the roughness reflects the dynamics of a growing surface.⁶ For example, in scanning tunneling microscopy (STM) or reflection high-energy electron diffraction observations on vicinal surfaces, the shape of the steps is reported to depend on the misorientation direction.^{7,8} Recently, quite high mobility samples (up to $1000 \text{ m}^2/\text{Vs}$) with thick spacer layers ($\sim 800 \text{ \AA}$) have been realized.^{9–11} We expect that the anisotropy of the surface structure is detectable in transport measurements on such a high mobility sample.

This paper concentrates on a low-temperature transport in modulation-doped heterostructures grown by molecular-beam epitaxy (MBE), which has a quite high mobility (μ) which ranges from 500 to $1100 \text{ m}^2/\text{Vs}$. We have observed that the heterostructures exhibit anisotropic low-temperature Hall mobilities. We examine the anisotropy of μ by postulating a model for the epitaxially grown heterointerface, assuming the formation of anisotropic islands. The transport properties of

two-dimensional electrons at the interface are calculated using Boltzmann’s equations and are compared with the experiments.

We have performed measurements of electron mobility in the $[\bar{1}10]$ and $[110]$ directions. The samples are modulation-doped $\text{Al}_x\text{Ga}_{1-x}\text{As}/\text{GaAs}$ heterostructures, grown by MBE on a (001) GaAs substrate (nominally no misorientations), with a 750-\AA spacer layer, as described in Ref. 11. The electron concentration N_s is about $1.3 \times 10^{15} \text{ m}^{-2}$ in the dark condition. We have found a large anisotropy of μ at 1.5 K between the two adjacent Hall bridges aligned in the $[\bar{1}10]$ and $[110]$ directions, i.e., $\mu_{[\bar{1}10]} > \mu_{[110]}$ as shown in Table I. The mobilities are isotropic at 77 K and the electron concentrations of these pairs of Hall bridges, estimated by Schubnikov–de Haas oscillations, are the same. The Hall bridge has a $400\text{-}\mu\text{m}$ -wide current channel with voltage probes separated by 1.5 mm.

This anisotropy is considered to stem from the anisotropy of the interface roughness because (i) no anisotropy of μ is observed when the ionized-impurity scattering is dominant, i.e., the electron concentration is low or the impurities are closer to the channel, and (ii) this anisotropy is very sensitive to the crystal growth conditions such as the As partial pressure or the growth temperature.⁶ The details of the growth condition dependencies will be reported elsewhere.

Consider a two-dimensional system confined in the z direction by a triangular potential. The scattering probability between the interface two-dimensional states \mathbf{k} and

TABLE I. Hall mobilities of $\text{GaAs}/\text{Al}_x\text{Ga}_{1-x}\text{As}$ two-dimensional electron gas measured at 1.5 K on two closely adjacent samples from the same wafer in two different directions, $[\bar{1}10]$ and $[110]$. The electron concentrations are for the dark and fully illuminated conditions.

| Sample number | n_s (10^{15} m^{-2}) | $\mu_{[110]}$ (m^2/Vs) | $\mu_{[\bar{1}10]}$ (m^2/Vs) | $\mu_{[\bar{1}10]}/\mu_{[110]}$ |
|------------------|------------------------------------|--|--|---------------------------------|
| A (illum. 1.5 K) | 2.4 | 668 | 1070 | 1.60 |
| A (dark 1.5 K) | 1.3 | 437 | 584 | 1.34 |
| B (illum. 1.5 K) | 2.6 | 997 | 1110 | 1.11 |
| B (dark 1.5 K) | 1.3 | 547 | 577 | 1.05 |
| B (illum. 77 K) | 2.6 | 20 | 20 | 1.0 |

\mathbf{k}' due to a fluctuation of the interface height $d(\boldsymbol{\rho})$ is given by the first Born approximation,³⁻⁵

$$Q^{\text{rough}}(\mathbf{k}, \mathbf{k}') = \frac{2\pi}{\hbar} \left\langle \left| \frac{e^2}{\kappa\epsilon(|\mathbf{k} - \mathbf{k}'|)} \left(\frac{1}{2}N_s + N_{\text{depl}} \right) \Delta_{\mathbf{k}-\mathbf{k}'} \right|^2 \right\rangle \times \delta(E_{\mathbf{k}} - E_{\mathbf{k}'}), \quad (1)$$

where N_{depl} is the fixed-charge concentration in the depletion layer, κ is the dielectric constant, and $\epsilon(q)$ is a correction factor derived using random-phase approximation. $\Delta_{\mathbf{q}}$ is the Fourier transform of the relative fluctuation $\Delta(\boldsymbol{\rho}) [= d(\boldsymbol{\rho}) - \langle d(\boldsymbol{\rho}) \rangle]$ and we introduce the interface correlation function G and its Fourier transform F ,¹³

$$G(\mathbf{a}) = \frac{1}{\Delta^2} \langle \Delta(\boldsymbol{\rho}) \Delta(\boldsymbol{\rho} + \mathbf{a}) \rangle, \quad (2)$$

$$F(\mathbf{q}) = \frac{1}{\Delta^2 \Lambda^2} \langle |\Delta_{\mathbf{q}}|^2 \rangle, \quad (3)$$

where Δ is the root mean square of $\Delta(\boldsymbol{\rho})$ and Λ is the lateral scale of the fluctuation. We described the roughening heterointerface as randomly distributed elliptical two-dimensional nucleations (islands) or holes with monolayer heights,

$$d(\boldsymbol{\rho}) = d_0 \sum_i \eta_i \theta [R_i^2 - (x - x_i)^2 - (1 + \epsilon)(y - y_i)^2], \quad (4)$$

where d_0 is a monolayer height [2.83 Å for GaAs (001)], ϵ (≥ 0) is the eccentricity of the islands, η is +1 (islands) or -1 (holes), and θ is a step function. R_i and (x_i, y_i) are the radius and center of the i th island. For simplicity, the eccentricity of the islands ϵ is assumed to be uniform, independent of size. This assumption may be too crude for a surface in equilibrium where the eccentricity should be smaller for smaller islands, since the surface energy is most important for small islands. However, STM measurements on monolayer step fronts have shown the existence of large anisotropy for small (< 100 Å) front undulations.⁷ This suggests that the growth surface is far from thermal equilibrium. In this model, Δ^2 is $d_0^2 n_I \pi \langle R^2 \rangle_g / \sqrt{1 + \epsilon}$, where n_I is the area concentration of the islands. Δ^2 / d_0^2 corresponds to a surface coverage C_v , if there is no overlapping of islands. We derive the average $\langle \cdots \rangle_g$ from the distribution of island radii $g(R)$. Although the actual shape of $g(R)$ is not known yet, we consider three possible functions,

$$\begin{aligned} g_a(R) &= \frac{2}{\Lambda^2} R e^{-(R/\Lambda)^2}, \\ g_b(R) &= \frac{2}{\sqrt{\pi}\Lambda} e^{-(R/\Lambda)^2}, \\ g_c(R) &= \frac{1}{\Lambda} \theta \left(1 - \frac{R}{\Lambda} \right). \end{aligned} \quad (5)$$

The correlation functions $F(\mathbf{q})$ for various distribution functions are shown in Fig. 1 for circular islands ($\epsilon = 0$).

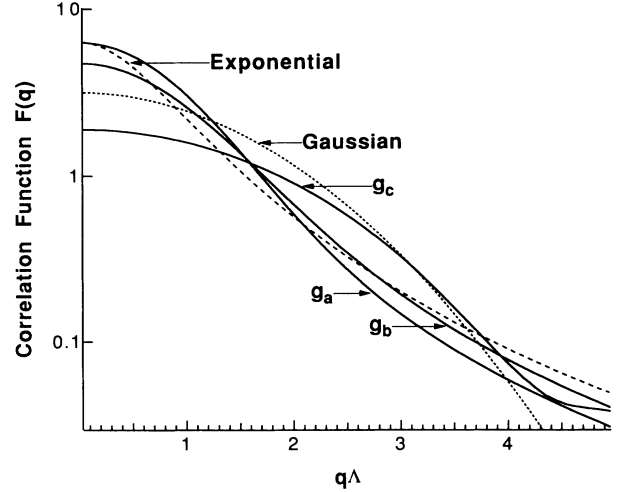


FIG. 1. Fourier-transformed surface-height correlation functions F for three distribution functions of islands radii, g_a , g_b , and g_c in Eq. (5) with no anisotropy. Conventional interface correlations models represented by Gaussian and exponential functions are also shown.

Conventional models of the interface roughness assume that $G(\mathbf{a})$ is Gaussian, $\exp[-(a/\Lambda)^2]$,^{1-5,12,13} or exponential, $\exp(-a/\Lambda)$.^{12,13} In Eq. (5), $g_a(R)$ represents a growth-interrupted (or thermal equilibrium) surface, where very small islands disappear since their surface energies are larger than the island formation energy, but this does not correspond to the current experimental situation. The conventional interface roughness model, represented by an exponential $G(\mathbf{a})$, is close to $g_b(R)$. $g_c(R)$, which is closer to the conventional Gaussian model, shows an extra oscillating structure due to sharp cutoff at $R = \Lambda$. We tentatively select $g_b(R)$ for the island distribution function in further calculations. If finite anisotropy is introduced, G and F also become anisotropic, where G is always larger and F is smaller in the direction parallel to the semimajor axis of the ellipse (the x direction, by definition, if $\epsilon > 0$) as shown in Fig. 2. This anisotropy of G can be understood by noting that the overlap of two ellipses displaced in the x direction is larger than that in the y direction, as shown in the inset of Fig. 2. Since mobility is roughly proportional to the inverse of $F(\mathbf{q})$, the mobility is always larger in the x direction than in the y direction.

Lateral growth is known to be faster in the $[\bar{1}10]$ direction in the current MBE growth conditions, which was confirmed by *in situ* STM observations⁷ or reflection high-energy electron diffraction.⁸ Therefore, we can assume that the island's radius is longer in the $[\bar{1}10]$ direction than in the $[110]$ direction, which is consistent with the anisotropy of the mobility.

Transport properties are calculated using a linearized form of Boltzmann's equation with ionized-impurity scattering also taken into account:

$$\left(-\frac{\partial f_0}{\partial E_{\mathbf{k}}} \right) e \mathbf{v}_{\mathbf{k}} \cdot \mathbf{E} = \frac{1}{(2\pi)^2} \int (g_{\mathbf{k}} - g_{\mathbf{k}'}) Q(\mathbf{k}, \mathbf{k}') d\mathbf{k}', \quad (6)$$

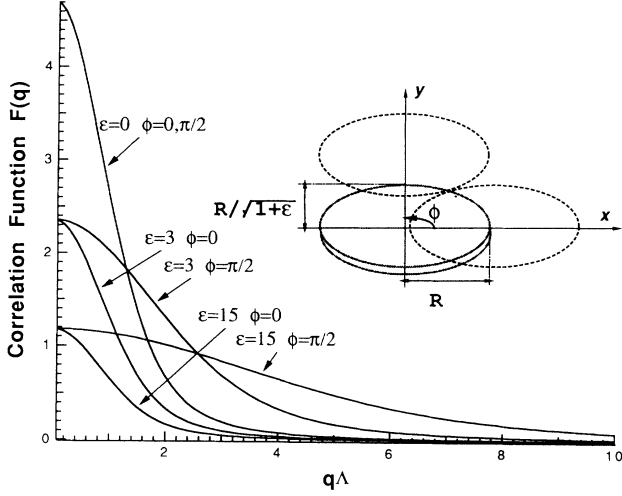


FIG. 2. Fourier-transformed surface-height correlation function F for circular ($\epsilon = 0$) and elliptical islands ($\epsilon = 3, 15$), in the semimajor axis direction ($\phi = 0$) and in the semiminor axis direction ($\phi = \pi/2$). $g_b(R)$ is used for the distribution of the island radii. $F(0) = \frac{3\pi}{2}/\sqrt{1+\epsilon}$. The inset shows the correlation (overlap) of the islands displaced by the same amount in the two directions.

$$g_k = \left(-\frac{\partial f_0}{\partial E_k} e v_k \right) \lambda(\theta) \cdot \mathbf{E}, \quad (7)$$

where f_0 is a Fermi distribution function. These reduce to two integral equations:

$$\cos \theta = \int_0^{2\pi} d\varphi [\lambda_x(\theta) - \lambda_x(\varphi)] \tilde{Q}(\theta, \varphi), \quad (8)$$

$$\sin \theta = \int_0^{2\pi} d\varphi [\lambda_y(\theta) - \lambda_y(\varphi)] \tilde{Q}(\theta, \varphi), \quad (9)$$

where

$$\tilde{Q}(\theta, \varphi) = \tilde{Q}^{\text{rough}}(\theta, \varphi) + \tilde{Q}^{\text{impurity}}(\theta - \varphi), \quad (10)$$

$$\tilde{Q}^{\text{rough}}(\theta, \varphi) = 2\pi \frac{\hbar}{m^*} \Delta^2 \Lambda^2 q_s^2 \left(\frac{1}{2} N_s + N_{\text{depl}} \right)^2 \frac{F(\mathbf{k} - \mathbf{k}')}{\epsilon(|\mathbf{k} - \mathbf{k}'|)^2}. \quad (11)$$

Here θ and φ are the angles of vectors \mathbf{k} and \mathbf{k}' relative to the x axis, q_s is the screening wave number ($m^* e^2 / 2\pi \hbar^2 \kappa$), k_F is the Fermi wave number, and m^* is the effective mass. These equations are solved by Fourier analysis to give mobilities in the two directions:

$$\mu_{xx} = \frac{e}{m^* \pi} \int_0^{2\pi} d\theta \lambda_x(\theta) \cos \theta, \quad (12)$$

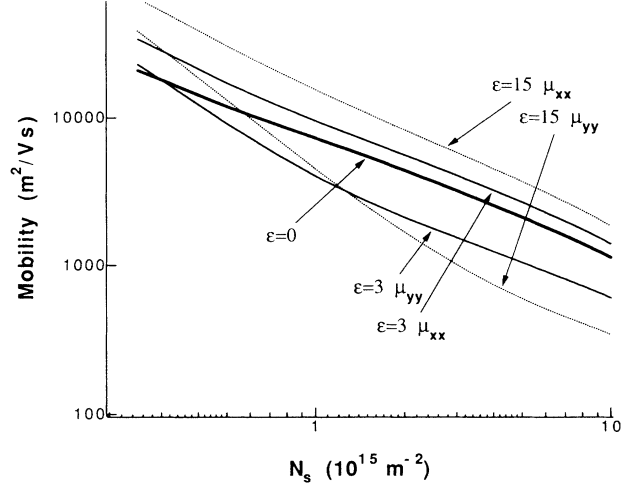


FIG. 3. Electron concentration vs the mobilities limited by roughness scattering in the two directions. The correlation length is 200 \AA and the coverage, $C_v = \Delta^2/d_0^2$, is 0.1.

$$\mu_{yy} = \frac{e}{m^* \pi} \int_0^{2\pi} d\theta \lambda_y(\theta) \sin \theta. \quad (13)$$

Figure 3 shows the calculated dependence of the anisotropic mobilities on electron concentration, determined by roughness scattering. The overall mobility is inversely proportional to a surface coverage C_v . The ra-

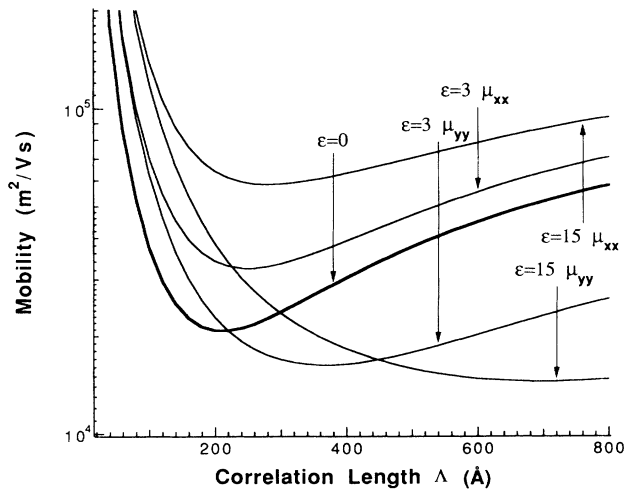


FIG. 4. Correlation length vs the mobilities limited by roughness scattering in the two directions. Electron concentration is $3.0 \times 10^{15} \text{ m}^{-2}$ and the coverage is 0.1.

tio of the anisotropy (μ_{xx}/μ_{yy}) decreases with decreasing electron concentration. The ratio also decreases with decreasing correlation length, as shown in Fig. 4. This is because $F(\mathbf{k} - \mathbf{k}')$ is highly isotropic if $|\mathbf{k} - \mathbf{k}'| \Lambda (< 2k_F\Lambda) \ll 1$. When $2k_F\Lambda \ll 1$, the mobilities of an anisotropic surface are larger than those of an isotropic surface for fixed C_v . Since $F \simeq \frac{3\pi}{2}/\sqrt{1+\epsilon}$ in this parameter range, as shown in Fig. 2, the mobility is proportional to $\sqrt{1+\epsilon}$. The mobilities reach a minimum when the correlation length is close to the Fermi wavelength ($\sim 400 \text{ \AA}$).

The mobilities limited by roughness scatterings and ionized-impurity scatterings are shown in Fig. 5 with the experimental results. We used the background charge concentration, $1 \times 10^{19} \text{ m}^{-3}$, determined from experiments on the samples with thinner spacers, where ionized-impurity scattering is dominant and the mobility is completely isotropic. The experimental results fit the calculation quite well when the eccentricity of the islands is assumed to be about 0.5–4 and $\Lambda \sim 200 \text{ \AA}$.

In conclusion, we have found the anisotropic electron mobility by low-temperature Hall measurements in a high-mobility modulation-doped $\text{Al}_x\text{Ga}_{1-x}\text{As}/\text{GaAs}$ heterostructure. The mobility anisotropy was explained by constructing an anisotropic interface roughness model as an ensemble of elliptic islands. In this model, the interface correlation function is close to exponential. The eccentricity and lateral scale of the islands are estimated

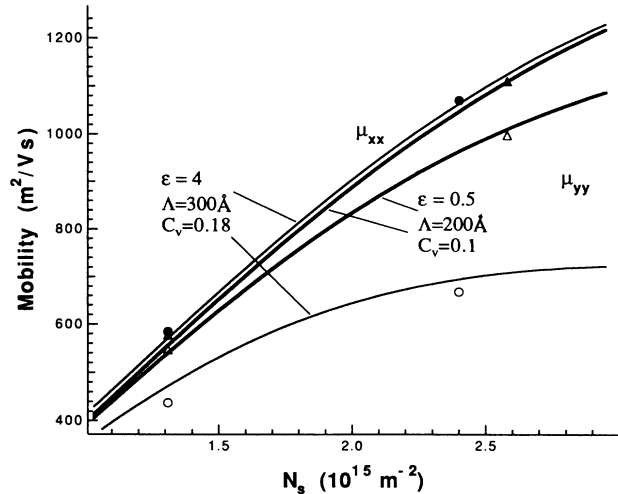


FIG. 5. Two sets of calculated mobilities limited by roughness scattering and ionized-impurity scattering, vs the electron concentration, and two experimental results, for sample A: $\mu_{[110]}$ (filled circle), $\mu_{[1\bar{1}0]}$ (open circle), and for sample B: $\mu_{[110]}$ (filled triangle), $\mu_{[1\bar{1}0]}$ (open triangle). The background uniform ion concentration is $1 \times 10^{19} \text{ m}^{-3}$.

by comparing the Boltzmann-type solution and the experimental results, and the concluded direction of the elliptic major axis is consistent with previously reported surface *in situ* measurements.

¹T. Ando, J. Phys. Soc. Jpn. **51**, 3900 (1982).

²Y. C. Cheng, in Proceedings of the 3rd Conference on Solid State Devices, Tokyo, 1971, edited by T. Arizumi [J. Jpn. Soc. Appl. Phys. Suppl. **41**, 173 (1972)]; Y. C. Cheng and E. A. Sullivan, Surf. Sci. **34**, 717 (1973).

³Y. Matsumoto and Y. Uemura, Jpn. J. Appl. Phys. Suppl. **2**, 367 (1974).

⁴T. Ando, J. Phys. Soc. Jpn. **43**, 1616 (1977).

⁵T. Ando, A. B. Fowler, and F. Stern, Rev. Mod. Phys. **54**, 437 (1982).

⁶Y. S. Fatt, J. Appl. Phys. **71**, 158 (1992). There is large amount of theoretical work, for example, M. Kardar, G. Parisi, and Y. Zhang, Phys. Rev. Lett. **56**, 889 (1986); J. G. Amar and F. Family, *ibid.* **64**, 543 (1990).

⁷M. D. Pashley, K. W. Haberern, and J. M. Gaines, Appl. Phys. Lett. **58**, 406 (1991).

⁸K. Ohta, T. Kojima, and T. Nakagawa, J. Cryst. Growth **95**, 71 (1989); P. R. Pukite, G. S. Petrich, S. Batra, and P. I. Cohen, *ibid.* **95**, 269 (1989).

⁹L. Pfeiffer, K. W. West, H. L. Stormer, and K. W. Baldwin, Appl. Phys. Lett. **55**, 1086 (1988).

¹⁰C. T. Foxon, J. J. Harris, D. Hilton, J. Hewelt, and C. Roberts, Semicond. Sci. Technol. **4**, 582 (1989).

¹¹T. Saku, Y. Hirayama, and Y. Horikoshi, Jpn. J. Appl. Phys. **30**, 902 (1991).

¹²D. Calecki, Phys. Rev. B **42**, 6906 (1990).

¹³G. Fishman and D. Calecki, Phys. Rev. B **43**, 11 581 (1991).

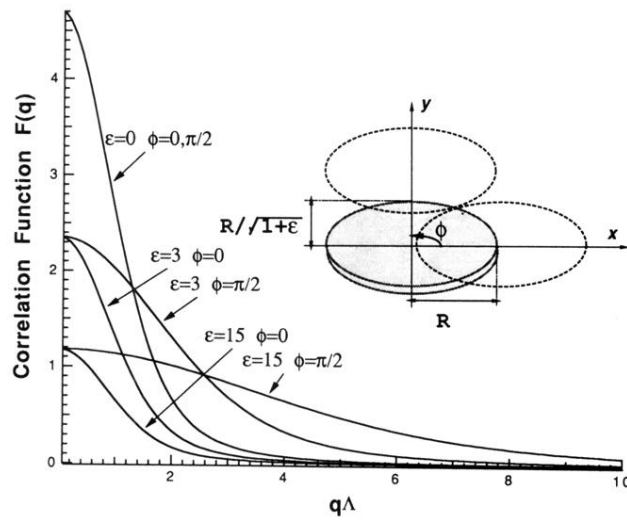


FIG. 2. Fourier-transformed surface-height correlation function F for circular ($\epsilon = 0$) and elliptical islands ($\epsilon = 3, 15$), in the semimajor axis direction ($\phi = 0$) and in the semiminor axis direction ($\phi = \pi/2$). $g_b(R)$ is used for the distribution of the island radii. $F(0) = \frac{3\pi}{2} / \sqrt{1 + \epsilon}$. The inset shows the correlation (overlap) of the islands displaced by the same amount in the two directions.